JOURNAL OF MATERIALS SCIENCE 29 (1994) 4875–4882

Effects of mechanical pressure on charge transport in some ferrocene derivatives in the presence of adsorbed vapours

A. BHATTACHARJEE, B. MALLIK*
Department of Spectroscopy, Indian Association for the Cultivation of Science, Jadavpur, Calcutta 700 032, India

The change in adsorption-induced electrical conductivity of some ferrocene derivatives as a function of temperature has been studied under moderate pressures. At a constant cell temperature, the conductivity of the pure ferrocene derivatives in the dry state depends on the applied pressure and this pressure dependence of conductivity is significantly different for different materials. A spectacular change in the electrical conductivity behaviour of these materials at the vapour-adsorbed state, as a function of temperature under mechanical pressure, has been observed. Pressure-induced change in conductivity of different ferrocene derivatives at the vapour-adsorbed state is remarkably different. The results have been discussed in the light of different existing theories. The unusual variation of conductivity with temperature under pressure is thought to be due to the phase transition in these materials.

1. Introduction

Ferrocene (*bis*(cyclopentadienyl)iron: $(C_5H_5)_2Fe$), the first synthesized organometallic sandwich compound, and its derivatives, are well known for their important electrochemical properties [1–4]. The technological usefulness of these materials have been recognized in different fields [5]. During the past three decades the effects of mechanical pressure upon the electrical conductivity of ferrocene (Fc–H) have been studied by different research groups and inconsistent results have been reported [6, 7] in the literature. The effects of pressure on the electrical conductivity of Fc–H were re-examined by Karvaly *et al.* [8] to determine the reason for the inconsistent results reported in the literature [6, 7]. From their experimental results, evidence was found of a slow and continuous phase transition in Fc–H under pressure at room temperature [8]. The two different current-pressure characteristic curves, as reported in the literature, were thought [8] to be dependent upon the prehistory of the sample. It was also proposed [8] that adsorption of minute amounts of moisture on Fc–H may cause additional effects on pressure dependence of the conductivity, particularly in the low-pressure region. It appeared that the systematic pressure-dependent conductivity studies in the low-pressure region, may provide new insight into both bulk and surface properties. Therefore, it was thought worthwhile to investigate the effects of mechanical pressure on the adsorption-induced electrical conductivity of Fc–H and its variation with temperature under carefully controlled conditions. We have already reported [9, 10] a drastic change in the adsorption-induced electrical conductivity of Fc–H with temperature under different pressures. To examine the effects of substitution groups (in the Fc–H unit) on the above-mentioned studies, similar experiments have been performed with some Fc–H derivatives. The results of the systematic studies on the effects of mechanical pressure on the adsorption-induced electrical conductivity of some Fc–H derivatives as a function of temperature are reported in this paper. The results have been compared with those for ferrocene.

2. Experimental procedure

The Fc–H derivatives used were ferrocene carboxylic-acid (Fc–COOH), acetyl ferrocene ($Fc–COCH_3$), ferrocene carbaldehyde (Fc–CHO) and benzoyl ferrocene ($Fc–COC_6H_5$). High-purity microcrystalline Fc–H derivatives (in powder form) were obtained from Aldrich Chemical Co. Inc. (Milwaukee, WI, USA) and were used after further purification by repeated crystallization. The chemical reagents used were of spectrograde or equivalent quality. The experiments were performed using a cylindrical pressure cell [10] placed inside a suitably designed conductivity chamber made of brass and fashioned with Teflon. Powder samples (30 mg) were loaded into the stainless steel pressure cell lined with an appropriate Teflon tubing and placed inside the chamber. The sample was evenly distributed over the base plate. The pressure-transducing piston was placed on the sample material. Teflon insulators were used at all critical places where

---

* Author to whom all correspondence should be addressed.

0022–2461

leakage could have interfered with the conductivity measurements. The base plate and the pressure transducing piston served as electrodes. The external mechanical pressure was created by placing different weights upon a platform, which exerted pressure on the pressure-transducing piston of the pressure cell. The temperature of the sample in the pressure cell was controlled by a proportional temperature controller (model RTE-110, Neslab Instruments Inc. Newington, NH, USA). The current was measured using an electrometer amplifier (model EA815, Electronic Corporation of India Ltd). The cell temperatures were recorded using a Panel Meter (model 2301, Hindusthan Instruments Ltd, India) using a copper–constantan thermocouple attached to the base plate of the pressure cell. Repeated heating and cooling of the sample in a dry nitrogen atmosphere ensured desorption of any preadsorbed vapour or gas. To allow various vapours inside the chamber, dry nitrogen gas was passed at a constant rate through a bubbler which contained the desired adsorbate chemical kept at a thermostatted bath to obtain a specific vapour pressure. Then, after exposure of the samples to the desired vapour at 5.33 kPa vapour pressure inside the chamber at 299 K for about 30 min (usual time for saturated adsorption), the adsorption was turned off. (At lower vapour pressures, most of the vapours do not show measurable change in the conductivity, so a higher value of vapour pressure was considered for the adsorption of different vapours to obtain an appreciable change in the adsorption-induced conductivity). The pressure-transducing piston was then slowly introduced into the cylindrical cavity and the pressure cell was then cooled to lower the cell temperature. The pressure was then applied. After allowing sufficient time (about 1 h) to attain equilibrium, the value of saturation current, I_s, was noted against a steady 40 V d.c. bias. The cell was then heated slowly and the current was noted with increasing temperature.

3. Results and discussion

3.1. Pressure-induced change in conductivity in the dry as well as vapour-adsorbed state

The effects of mechanical pressure, P, on the dark conductivity, σ (proportional to current), of dry Fc–H and its derivatives at a constant temperature are shown in Fig. 1. In the case of dry Fc–H, the logarithm of dark current increased slightly for the very initial low pressurizations, but it remained almost independent of further pressurizations. For the dry Fc–COOH, variation of logarithm of current was almost independent of applied mechanical pressure for the entire pressure range. In the case of Fc–$COCH_3$ in the dry state, the logarithm of current increased sharply with initial pressurizations and then it increased slowly with further pressurization. For the dry Fc–COC_6H_5 the logarithm of current was almost unchanged for the first pressurization, but it decreased for further low pressurizations up to about 1 MPa, then remained almost independent of pressure up to about 2.5 MPa and on further pressurizations above 2.5 MPa the value of the logarithm of current increased gradually. From Fig. 1 it is clear that the pressure-induced change in conductivity of the Fc–H derivatives in the dry state depends significantly on the nature of the derivatives used, particularly in the lower pressure region. At pressures above 0.97 MPa, the variation in logarithm of current against pressure for the dry materials is relatively systematic. At the vapour adsorbed state under pressure, Fc–CHO turned to a sticky material. Therefore, this material could not be used for the present study.

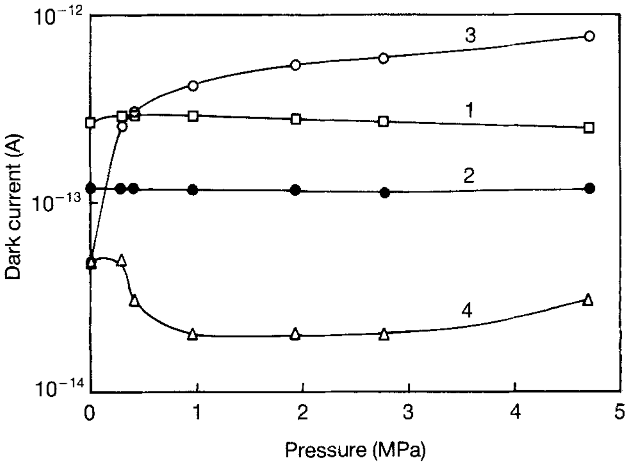

Figure 1 The plots of log dark current versus pressure for Fc–H (cell temperature 288 K) and its derivatives (cell temperature 299 K) in the pure and dry state: (1) Fc–H, (2) Fc–COOH, (3) Fc–$COCH_3$ and (4) Fc–COC_6H_5.

It has already been mentioned in our earlier communications [11, 12] that, in general, ethanol vapour is very sensitive to the adsorption-induced changes in the electrical conductivity of Fc–H and its derivatives. Therefore, ethanol vapour was chosen for detailed experiments on different materials. The effects of mechanical pressure on the dark conductivity of Fc–H and its derivatives at a constant temperature with adsorbed ethanol vapour, is shown in Fig. 2 in which plots of logarithm (I_{ADS}/I_{DRY}) for the materials under study against applied mechanical pressure are given, where I_{ADS} is the adsorption-induced electrical current at a certain temperature and applied pressure, and I_{DRY} corresponds to the electrical current of the dry material at the same temperature and applied pressure. Adsorption-induced (with ethanol vapour) conductivity of Fc–H increases slowly with increasing pressurization (Fig. 2). In the Fc–H derivatives with adsorbed ethanol vapour at the same vapour pressure, a significant variation in the adsorption-induced conductivity with applied pressure has been observed (Fig. 2). The plots of (I_{ADS}/I_{DRY}) versus pressure are different for different materials adsorbed with ethanol vapour at the same vapour pressure (Fig. 2). From Fig. 2 it is seen that at pressures above 0.97 MPa, variation in log(I_{ADS}/I_{DRY}) with pressure is systematic. The pressure dependence of the conductivity of the powdered materials subjected to low compressions is usually determined by the number and the area of the grain-boundary regions connecting the particles [13].

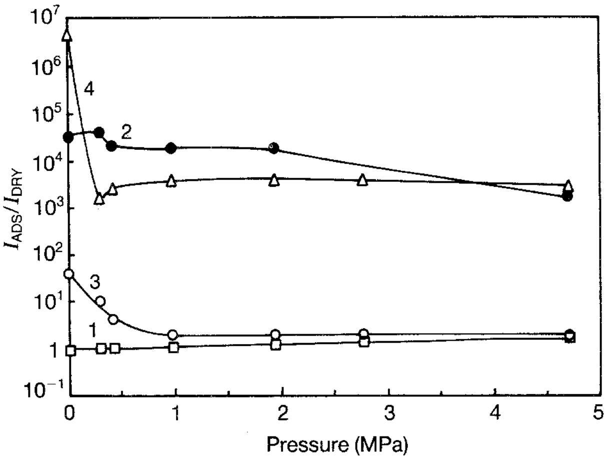

Figure 2 The plots of log (I_{ADS}/I_{DRY}) versus pressure for Fc–H (cell temperature 288 K) and its derivatives (cell temperature 299 K) in the ethanol adsorbed state: (1) Fc–H, (2) Fc–COOH, (3) Fc–$COCH_3$ and (4) Fc–COC_6H_5.

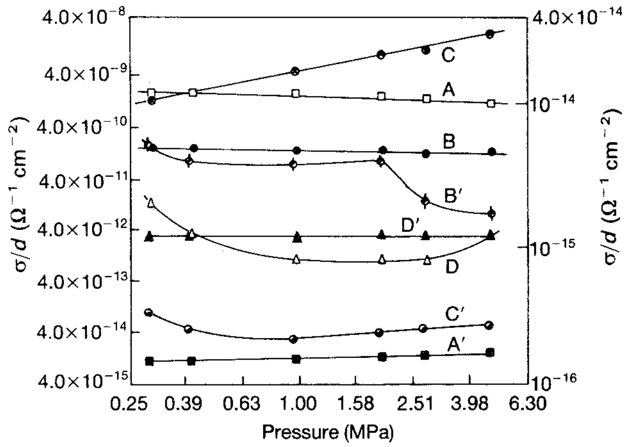

Figure 3 The log (σ/d) versus log p (pressure) plots for Fc–H (cell temperature 288 K) and its derivatives (cell temperature 299 K) in the pure and dry state, and the ethanol vapour adsorbed (at 5.33 kPa vapour pressure) state. (A) Dry state of Fc–H; (A′) vapour-adsorbed state of Fc–H; (B) dry state of Fc–COOH; (B′) vapour-adsorbed state of Fc–COOH; (C) dry state of Fc–$COCH_3$; (C′) vapour-adsorbed state of Fc–$COCH_3$; (D) dry state of Fc–COC_6H_5; and (D′) vapour-adsorbed state of Fc–COC_6H_5. Left scale for vapour-adsorbed states; right scale for dry states.

Thus the conductivity of polycrystalline powdery materials is expected to exhibit qualitatively a characteristic pressure dependence: a considerable increase with increasing pressure at low compression. In the present case, although this prediction is valid for Fc–H, the data obtained for the Fc–H derivatives in most cases (particularly in the adsorbed state and also in dry Fc–COC_6H_5) do not agree with this prediction. Data presented here have not been corrected for the pressure-induced change in the sample geometry, primarily in thickness. Measurement of the pressure-induced change in sample thickness is very difficult. To have an idea about the effects of pressure-induced change in the thickness of the sample cell on the conductivity, log (σ/d) values (both in the dry as well as vapour-adsorbed states) have been plotted against log pressure (Fig. 3), where $\sigma/d = I/AV$, with d the thickness of the sample cell, I the current at a particular pressure and temperature, A the area of the sample cell, and V the applied voltage across the electrodes. From Fig. 3, it is seen that the factor σ/d is nearly independent of pressure for the dry Fc–H (Curve A) and Fc–COOH (Curve B). In the case of dry Fc–$COCH_3$, the value of σ/d increases linearly with increasing pressure as observed from curve C. Dry Fc–COC_6H_5 shows an entirely different kind of variation of σ/d with pressure: initially it decreases with increasing pressure and at higher pressures it increases with pressure (Curve D, Fig. 3). In the case of ethanol vapour adsorption on Fc–H, σ/d increases with increasing pressure, as observed from curve A′ in Fig. 3. For Fc–COOH with adsorbed ethanol vapour, the variation of σ/d factor with applied pressure (Curve B′, Fig. 3) is not smooth; on application of pressure, initially σ/d decreases with pressure, then remains constant with increasing pressure, and at higher pressures, σ/d again decreases with increasing pressurization. In the case of Fc–$COCH_3$, with adsorbed ethanol vapour, a decrease in the value of σ/d with increasing pressurization at lower pressures has been observed (Curve C′, Fig. 3), whereas at higher pressures, the value of σ/d increases with increasing pressure. As mentioned earlier, for Fc–COC_6H_5, the value of σ/d is highly sensitive to pressure in the dry state, but with adsorbed ethanol vapour, the value of σ/d is almost independent of pressure (Curve D′, Fig. 3). Thus, the results indicate that the pressure-dependence of the factor σ/d is significantly different for different materials both in the dry and vapour adsorbed state. The value of σ/d depends on the pressure-induced change in the sample thickness, d, and also on the pressure-induced change in the conductivity, arising from solid vapour interaction (for adsorbed states) under pressure. It is believed that the conductivity/current against pressure diagram reflects the fundamental material properties of the powdery materials. The conductivity change due to adsorption for many powdery materials has been well studied [14–16]. Thus, the observed results of the pressure-dependence of conductivity of Fc–H and its derivatives appear to be due to compaction and related pressure-induced changes in the contact areas at grain boundaries, pressure-induced other changes in the materials, and the pressure-sensitive conductivity components related to the vapour adsorbed on or bound to the molecules of the corresponding materials.

We have reported a drastic change in the shape of the plot of log current versus reciprocal temperature as a function of applied mechanical pressure for Fc–H [9, 10]. Similar to the case of Fc–H, for the Fc–H derivatives with adsorbed ethanol vapour, spectacular pressure-induced changes in the shape of the log current/conductivity versus reciprocal temperature curves have also been observed, as shown in Fig. 4 for Fc–COOH. In the case of Fc–COOH, application of initial pressure of 0.16 MPa (Curve 3, Fig. 4) decreases the current at lower as well as higher temperatures, but the shape of conductivity versus reciprocal temperature curve remains almost the same. For some higher pressures (0.87 and 1.94 MPa, curves 4 and 5,

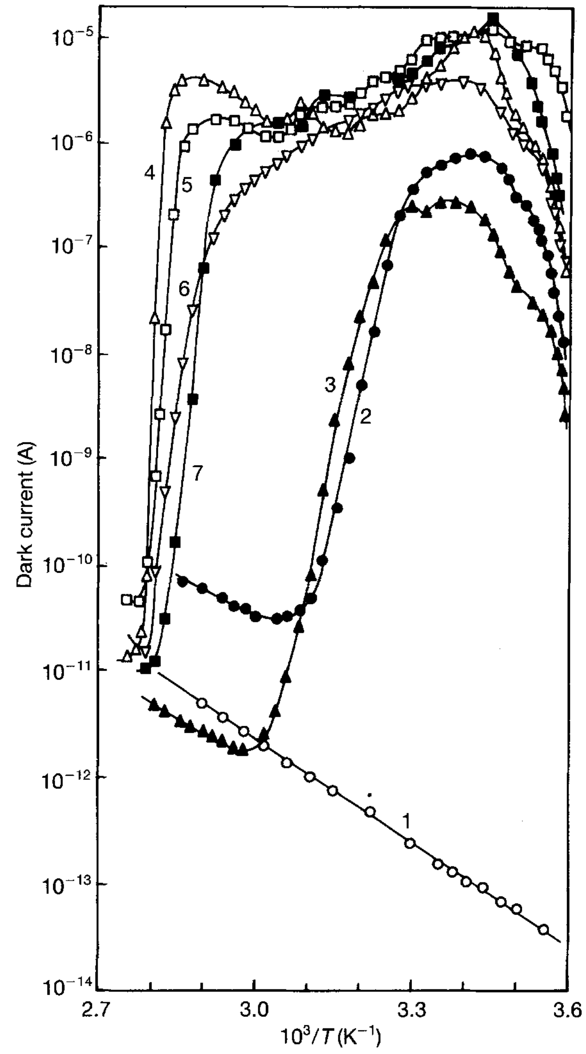

Figure 4 The plots of log dark current versus reciprocal temperature for Fc–COOH cells adsorbed with ethanol vapour at 5.33 kPa vapour pressure under different applied mechanical pressures. (1) Pure and dry material under no pressure; (2) adsorbed material under no pressure; (3) 0.16 MPa; (4) 0.97 MPa; (5) 1.94 MPa; (6) 2.77 MPa; (7) 4.71 MPa.

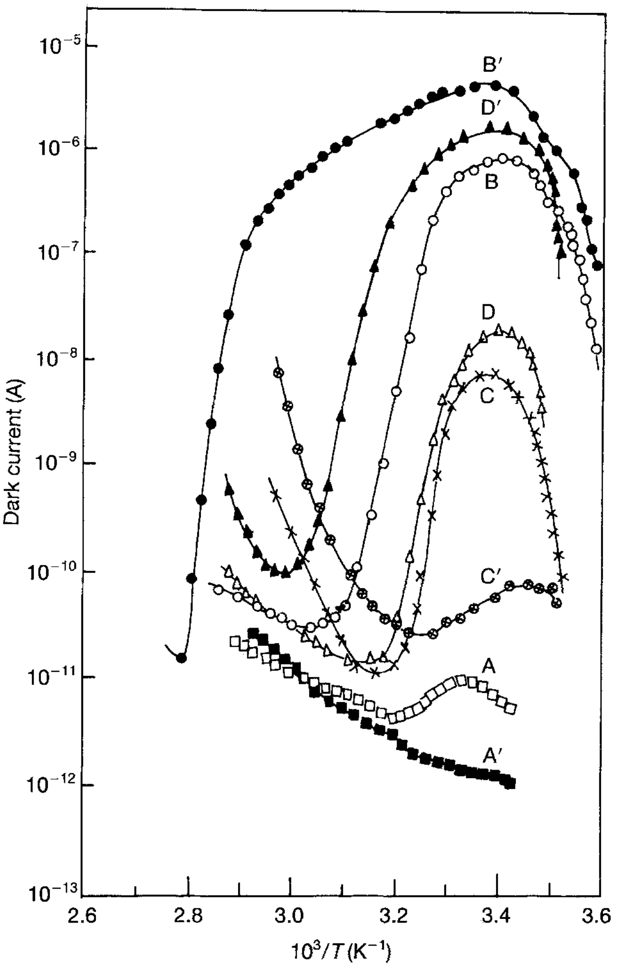

Figure 5 Plots of log dark current versus reciprocal temperature for Fc–H and its derivatives adsorbed with ethanol vapour at 5.33 kPa vapour pressure in the pressure-free state and under a pressure of 2.77 MPa. (A) Fc–H in the pressure-free state; (A′) Fc–H under pressure; (B) Fc–COOH in the pressure-free state; (B′) Fc–COOH under pressure; (C) Fc–$COCH_3$ in the pressure-free state; (C′) Fc–$COCH_3$ under pressure; (D) Fc–COC_6H_5 in the pressure-free state; (D′) Fc–COC_6H_5 under pressure.

respectively) an additional strong peak has been observed in the higher temperature region. Such pressure-induced changes in the shape of the logarithm of conductivity versus reciprocal temperature curves are different for the different Fc–H derivatives. On application of a fixed value of pressure on different Fc–H derivatives, under identical adsorbed conditions, the shapes of the log conductivity versus reciprocal of temperature curves are observed to be significantly different, as shown in Fig. 5. From Fig. 5 it is seen that in the case of Fc–H and Fc–$COCH_3$ conductivity under pressure (2.77 MPa) decreases (curves A′ and C′, respectively) significantly (particularly at lower temperatures) from that of the values under no external pressure (Curves A and C, respectively). On the other hand, in the case of Fc–COOH and Fc–COC_6H_5 conductivity under the same amount of pressure (Curves B′ and D′, respectively, Fig. 5) increases drastically from the corresponding values under no external pressure over the entire temperature range (Curves B and D, respectively). Similar to Fc–H [9, 10], for its derivatives, humps/broad bands also appear at certain values of pressure and disappear at some higher pressure. The appearance and disappearance of the humps/broad bands under pressure depend spectacularly on the nature of the Fc–H derivatives used. The difference in the shape of the logarithm of conductivity versus reciprocal temperature plots (as shown in Fig. 5) arises from the differences in the interaction of the vapour molecules with various functional groups attached to the ferrocene unit. The interaction of a particular vapour with Fc–H and its derivatives will be discussed later.

It has already been reported [11, 12] that conductivity peaks appeared on heating sandwich cells of Fc–H and its derivatives in the ethanol adsorbed state (under a clipping pressure of 0.035 MPa). Although those results were obtained under different experimental conditions compared to the present case, a close relationship exists between the cases; a conductivity peak appears in both the cases. In the present case, the applied mechanical pressure influences the conductivity–temperature behaviour. The intensity, I_{max}, of the above-mentioned conductivity peak and the temperature, T_{max}, at which the main peak/hump appears, depend on the applied pressure. On application of a fixed value of pressure upon different materials under identical adsorbed conditions, the values of I_{max} and T_{max} were observed to be different (Fig. 5) for different materials. No regular variation of I_{max} with pressure was observed in the case of either Fc–H or its derivatives. The value of I_{max} in the higher pressure region was found to increase with increasing pressure in case of Fc–COOH (Fig. 4), while a decrease was noticed in the case of Fc–$COCH_3$ and Fc–COC_6H_5. In the case of either Fc–H or its derivatives, I_s did not show any regular variation with pressure over the entire pressure region. The change in T_{max} with pressure for Fc–H and Fc–COC_6H_5 was very small, while for others the change was appreciable. The values of I_s, I_{max} and T_{max} under different pressures on the Fc–H derivatives with adsorbed ethanol vapour at 5.33 kPa vapour pressure are shown in Table I. The differences in the conductivity versus reciprocal temperature diagrams for each individual material at the adsorbed state under pressure are due to pressure-induced modifications.

3.2. Pressure-induced change in activation energy of Fc–H and its derivatives in the vapour-adsorbed state

Dark conductivity in organic and organometallic materials is usually expressed by the Arrhenious relation [14, 16, 17]

$$\sigma(T) = \sigma_0 \exp[-E/2kT] \qquad (1)$$

where $\sigma(T)$, σ_0, E, k and T have their usual meanings. The values of E (E_L at lower temperature and E_H at higher temperature) have been estimated from the conductivity versus reciprocal temperature plots. An interesting variation in the E values under different pressures has been obtained and this is shown in Figs 6 and 7. The variations of E_L and E_H for Fc–H with pressure are very similar at higher pressures. But it is clear that the lower pressurizations cause enormous changes in the calculated activation energy values and thus in dark conduction properties. The variation of E_L with pressure is significantly different from the variation of E_H with pressure in the case of Fc–H derivatives (Figs 6 and 7). In some cases (mainly for E_H in the case of Fc–COOH), the values of E could not be calculated owing to the limited number of data points in the temperature region of interest. As the heating rate and the method of experiment are the same for all sets of experiments, it appears that the change in E values for these materials in the adsorbed state is solely due to the interaction between the adsorbent and adsorbate under different pressures.

TABLE I The values of I_s, I_{max} and T_{max} under different pressures on various ferrocene derivatives adsorbed with ethanol vapour at 5.33 kPa vapour pressure

Ferrocene derivatives studied	Pressure (MPa)	I_s (A)	I_{max} (A)	T_{max} (K)
Fc–COOH	0	2.4×10^{-8}	8.2×10^{-7}	293.05
	0.16	8.2×10^{-9}	2.8×10^{-7}	297.45
	0.97	1.9×10^{-7}	1.2×10^{-5}	292.20
	1.94	1.9×10^{-6}	1.2×10^{-5}	290.50
	2.77	1.4×10^{-7}	3.8×10^{-6}	299.75
	4.71	3.3×10^{-7}	1.5×10^{-5}	290.00
Fc–$COCH_3$	0	7.5×10^{-11}	9.1×10^{-9}	291.00
	0.42	7.6×10^{-10}	6.5×10^{-10}	291.00
	0.97	3.2×10^{-10}	3.3×10^{-8}	291.00
	1.94	1.5×10^{-9}	1.0×10^{-6}	290.75
	2.77	4.0×10^{-11}	6.5×10^{-11}	285.80
	4.71	1.1×10^{-11}	1.3×10^{-11}	286.00
Fc–COC_6H_5	0	3.0×10^{-9}	2.5×10^{-8}	289.50
	0.42	2.4×10^{-6}	4.2×10^{-6}	289.00
	0.97	2.5×10^{-9}	1.1×10^{-8}	288.00
	1.94	1.0×10^{-8}	3.3×10^{-6}	290.50
	2.77	5.0×10^{-7}	2.7×10^{-6}	290.00
	4.71	1.5×10^{-8}	2.3×10^{-7}	290.00

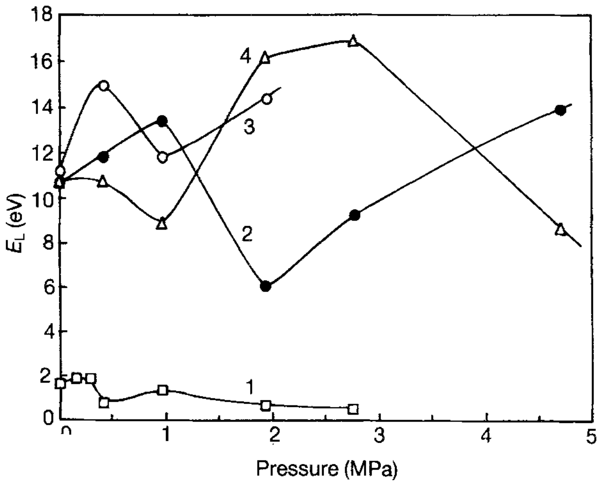

Figure 6 The plots of E_L versus pressure for Fc–H and its derivatives with adsorbed ethanol vapour at 5.33 kPa vapour pressure. (1) Fc–H; (2) Fc–COOH; (3) Fc–$COCH_3$; (4) Fc–COC_6H_5.

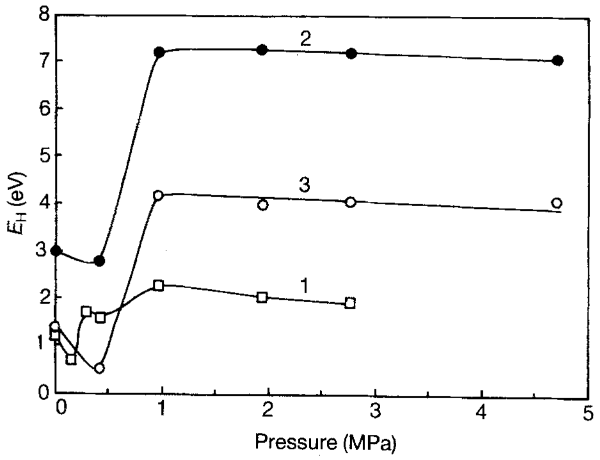

Figure 7 Plots of E_H versus pressure for Fc–H and its derivatives with adsorbed ethanol vapour at 5.33 kPa vapour pressure. (1) Fc–H; (2) Fc–$COCH_3$; (3) Fc–COC_6H_5.

3.3. Effects of the nature of the adsorbates on the pressure-induced change in conductivity and other associated parameters

To study the effect of the nature of the adsorbates on the pressure-induced change in conductivity and other associated parameters, experiments were undertaken for all materials under study with different adsorbed vapours (e.g. 2-propanol, ethyl acetate, carbon tetrachloride, etc.) at the same vapour pressure under constant mechanical pressure. The results observed for Fc–COOH are shown in Fig. 8. It is interesting to note that additional conductivity peaks/humps are observed in the conductivity versus reciprocal temperature plot (Fig. 8) for Fc–COOH with adsorbed ethanol and benzene vapours under a constant mechanical pressure of 0.16 MPa. But no such hump/peak is observed for adsorption of 2-propanol, methanol and carbon tetrachloride vapours. In general, the nature of the adsorbed vapours plays an important role in the changes of shape of the conductivity versus reciprocal temperature plots at a fixed value of applied pressure on a particular Fc–H derivative, and this is evident from Fig. 8. Similarly, the effects of the nature of the adsorbed vapours for the pressure-induced changes in the shape of the conductivity versus reciprocal temperature plots for the other Fc–H derivatives were significant. The effects of the nature of the adsorbed vapours on the values of I_s, I_{max}, T_{max}, E_L and E_H under a fixed pressure on a particular Fc–H derivative in the adsorbed state, are shown in Table II. The evaluated E values characterize the dependence of the adsorbate–adsorbent complex system upon the nature of the adsorbates under constant pressurization.

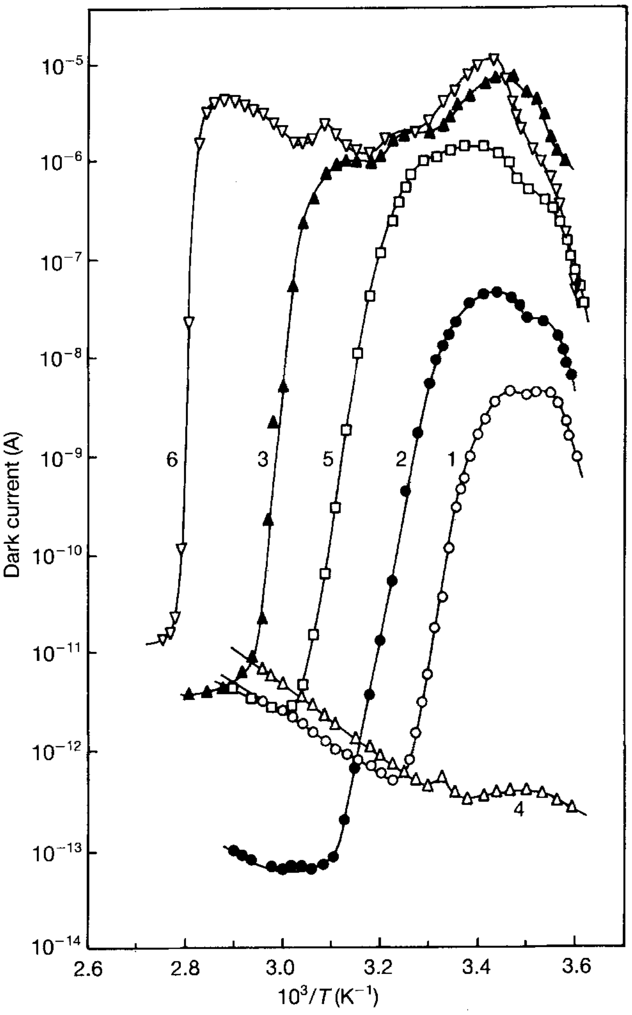

Figure 8 Plots of log dark current versus reciprocal temperature for Fc–COOH cells under the same pressure of 0.97 MPa, adsorbed with different vapours at 5.33 kPa vapour pressure. (1) carbon tetrachloride; (2) methanol; (3) benzene; (4) ethyl acetate; (5) 2-propanol; (6) ethanol.

From the experiment with sandwich cells (clipping pressure of 0.035 MPa) of these materials it has been observed that methanol is less sensitive to the adsorption-induced changes in conductivity. Although 2-propanol is quite sensitive to most of the materials studied, it is almost insensitive to Fc–$COCH_3$. Ethyl acetate vapour is not sensitive to adsorption-induced changes in the conductivity of Fc–COC_6H_5. But the sensitivity of ethyl acetate vapour is significant to adsorption-induced changes in Fc–COOH. Thus, the selectivity (specificity) in the interaction of vapours with the different ferrocene derivatives is evident from the observed results [12].

3.4. Discussion of the pressure-induced change in conductivity as well as activation energy of the materials

The effect of pressure on the conductivity of semiconducting powdered materials has been reported by several authors [8, 18–23] and we have discussed this in an earlier communication [10]. Our observations of the linear relationship of log conductivity with applied pressure in some cases agrees with Boon's prediction [21] (log conductivity proportional to applied pressure) for pressure dependence of conductivity in the case of materials of lower dielectric constant. Other commonly used theories, such as the formation of charge-transfer (CT) complexes [24, 25] of the solid materials with the adsorbed vapour molecules, change in dielectric constant of the materials due to physical mixing with the vapour molecules [26, 27], change in

TABLE II The values of I_s, I_{max}, T_{max}, E_L and E_H under 0.97 MPa pressure on Fc–COC_6H_5 adsorbed with different vapours at 5.33 kPa vapour pressure

Vapours used	I_p[a] (eV)	E_A[a] (eV)	DC[a]	I_s (A)	I_{max} (A)	T_{max} (K)	E_L (eV)	E_H (eV)
Benzene	9.24	2.46	2.27	1.3×10^{-9}	7.9×10^{-9}	288.6	10.54	5.65
Ethanol	10.50	0.59	24.0	2.5×10^{-9}	1.1×10^{-8}	288.0	8.86	4.19
2-propanol	10.79	0.67	18.30	1.0×10^{-7}	7.1×10^{-7}	289.5	13.92	4.93
Methanol	10.85	0.38	32.63	8.0×10^{-9}	5.0×10^{-8}	289.3	8.12	8.86
Carbon tetrachloride	–	1.21	2.23	5.0×10^{-8}	2.0×10^{-6}	289.75	15.00	1.82

[a] I_p = ionization potential; E_A = electron affinity; DC = dielectric constant. References for the values of I_p, E_A and DC are given in [11, 12].

polarization energy [23] due to pressurization, may explain the pressure-induced change in conductivity as well as activation energy of the materials. In favour of the formation of CT complexes, the semiconduction activation energy should decrease gradually with initial increasing pressure and ultimately attain almost a saturation value against further increasing pressure [18, 27]. However, our results (Figs 6 and 7) do not agree with this prediction. For the formation of CT complexes under a particular pressure, the current enhancement (i.e. saturation current, I_s) should show a linear relationship with either the ionization potential or the electron affinity of the vapours used [15]. Our results do not show (as in Table II) such a relationship, which excludes the possibility of the formation of CT complexes. If the conductivity change in Fc–H and its derivatives with adsorbed vapours and under moderate pressure is due to the physical mixing of vapours with solid molecules, a relationship between I_s and dielectric constant of the vapours used, and also between E and dielectric constant, is expected. Such a relationship has not been found to exist between the saturation current, I_s, after pressurization (and also E) in the adsorbed state and the dielectric constant of the vapours used (Fig. 9 and Table II). Thus, the theory of change in dielectric constant in the adsorbed state is not suitable for explaining the observed results regarding the pressure-induced changes in conductivity of Fc–H and its derivatives in the vapour-adsorbed state. Batley and Lyons [23] reported that the decrease in volume at high pressure will produce an increase in the polarization energy with a consequent decrease in E. Thus, E values obtained from the slopes of the conductivity versus reciprocal temperature plots under pressure should have a linear relationship with the pressures applied. However, no such relationship has been observed, as is evident from Figs 6 and 7.

Pure Fc–H derivatives undergo various kinds of mesophase transitions associated with the intermolecular interactions [28–31]. It is known that the controlled introduction of adsorbate into a molecular matrix may affect phase transition in organic solids and drastically change the electrical conductivity [32]. An adsorption-induced reversible structural phase transition in the materials under study at suitable temperatures has also been established recently [11, 12]. Thus on the basis of this evidence it is suggested that Fc–H derivatives, similar to Fc–H in the vapour-adsorbed state, undergo phase transition, which is modified by both temperature and pressure, and this is manifested in the unusual variation of conductivity with temperature under different values of applied pressure. We have mentioned earlier that in the vapour-adsorbed state under pressure, Fc–CHO turned into a sticky material. It has been reported [28] that pure Fc–CHO shows structural phase transition at 317 K. Possibly in the vapour-adsorbed state under pressure such a phase transition occurs in this material at a relatively lower temperature and, as a result, the material becomes sticky, as observed in pure Fc–CHO above 317 K [28].

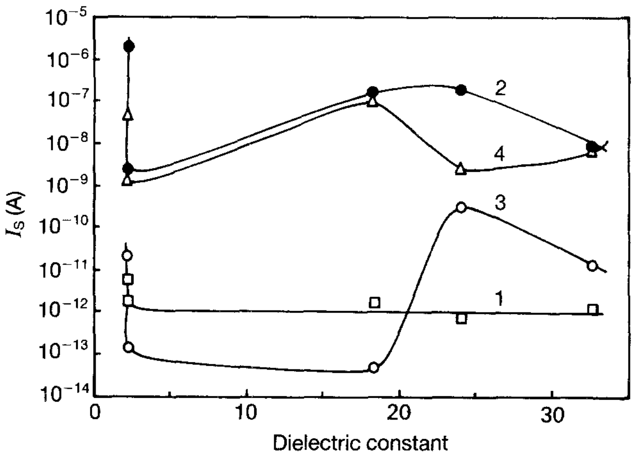

Figure 9 Plots of I_S versus dielectric constant of the vapours used, for Fc–H (cell temperature 288 K; pressure 0.16 MPa) and its derivatives (cell temperature 299 K; pressure 0.97 MPa) with adsorbed vapours at 5.33 kPa vapour pressure. (1) Fc–H; (2) Fc–COOH; (3) Fc–$COCH_3$; (4) Fc–COC_6H_5.

The adsorption-induced phase transition depends [11, 12] on the nature of the adsorbed vapours and also on the substituent group in a particular Fc–H derivative. It has been reported that the cooperative interaction which determines the phase transition is very complicated in nature [28, 31]. Application of mechanical pressure to the sample cell causes a change in the cooperative interaction in the solid–vapour system and consequently, the situation becomes more complicated.

3.5. Interaction of Fc–H derivatives with vapours and the pressure-induced modification

Ferrocene is a simple organometallic complex which may be formally considered in terms of two coplaner cyclopentadienyl rings lying above and below a central iron. It is also considered that the two cyclopentadienyl rings of the Fc–H unit rotate with respect to each other about the fixed central iron. But recently, Medina *et al.* [33] have reported that the two coplaner cyclopentadienyl rings of ferrocene unit may rotate with respect to each other about the central iron as if the metal acts as a "ball bearing" between two plane surfaces. Thus, in the case of functionalized ferrocenes, a wide range of relative orientations of the substituents may be achieved. The primary interaction of a ferrocene derivative with the vapour molecules is mainly between the functional groups attached to the ferrocene unit and the vapours, but a number of other features increase the specificity. It is well known that the binding of different small molecules with proteins and enzymes is very specific and the foreign molecules are accommodated in a particular conformation (among many possible conformations) of proteins and enzymes [34]. In fact, this particular conformation (equilibrium conformation) is induced by the binding molecules [34]. The idea of conformational changes upon substrate binding to optimize that binding can be applied to the case of binding of vapour molecules with ferrocene derivatives having a wide range of relative orientations of the substituents. In this case, the correct spatial arrangement of the substituents may be induced by the vapour molecules, which will organize the functional groups of the ferrocene derivatives in an optimal manner by selective rotation of the cyclopentadienyl rings. Only a proper (correct) vapour can selectively organize the ferrocene derivatives to the correct equilibrium conformation, forming a solid–vapour complex. The selectivity in the interaction of various vapours with a particular ferrocene derivative arises from the differences in the binding affinities of vapour molecules to specific regulatory (binding) sites among different possible conformations which modulate the equilibrium conformation. Pressure has been proved to be an extremely powerful variable in changing the density of matter. As the density of a material is increased due to pressurization, the electronic systems binding its atoms together become strained and deformed. Sometimes the systems adjust by switching abruptly to different configuration with lower free energy, and in doing so the electrical conductivity may change markedly [35]. Temperature is also a variable used to perturb the electronic systems. In general, the effect of increased temperature is to increase the amplitude of the thermal motion of atoms and to decrease the density. Sometimes the combined (rather competing) effect of pressure and temperature can throw a system into a different structural mode, with consequent changes in the electrical conductivity behaviour [35]. The externally applied mechanical pressure affects drastically the "ball-bearing" motion of the cyclopentadienyl rings of the ferrocene unit and influences the binding properties of the adsorbed vapour molecules and their physical state with a consequent change in the equilibrium conformation of the ferrocene derivative. A change in conductivity of the material at the adsorbed state under pressure arises due to the reorientation of the adsorbed vapour molecules along the charge transport routes. With changing temperature, under a fixed pressure, a change in equilibrium conformation of the solid, and hence a change in binding sites for the vapour molecules, leads to a change in the conductivity versus temperature profile depending on the nature of the adsorbed vapour upon a ferrocene derivative.

It was mentioned in the previous section that application of mechanical pressure causes a change in cooperative interaction (which determines phase transition) in the solid–vapour system. The reason for the pressure-(as well as temperature)-induced change in cooperative interaction is understandable from the above discussion.

Acknowledgement

Authors thank Professor T. N. Misra, Head of the Department of Spectroscopy, for his interest in their work.

References

1. A. P. F. TURNER, I. KARUBE and G. S. WILSON, "Biosensors" (Oxford University Press, Oxford, New York, Tokyo, 1987).
2. X. B. WANG, C. D'SILVA and R. PETHIG, *J. Mol. Electron.* **6** (1990) 129.
3. M. H. SMIT and A. E. G. CASS, *Anal. Chem.* **62** (1990) 2429.
4. B. W. ROCKETT and G. MARR, *J. Organomet. Chem.* **416** (1991) 327.
5. C. E. CARRAHER, J. E. SHEETS and C. U. PITTMAN, "Advances in Organometallic and Inorganic Polymer Science" (Marcel Dekker, New York, Basel, 1982).
6. Y. OKAMOTO, J. Y. CHANG and M. A. KANTOR, *J. Chem. Phys.* **41** (1964) 4010.
7. A. V. MAKSIMUCHEV, V. A. ZHORIN, A. T. PONOMERENKO and N. S. ENIKOLOPJAN, *Dokl. Phys. Chem. Akad. Nauk SSSR* **241** (1978) 593.
8. B. KARVALY, B. MALLIK and G. KEMENY, *J. Mater. Sci. Lett.* **4** (1985) 912.
9. A. BHATTACHARJEE and B. MALLIK, *ibid.* **11** (1992) 35.
10. *Idem, J. Mater. Sci.* **27** (1992) 5877.
11. B. MALLIK and A. BHATTACHARJEE, *J. Phys. Chem. Solids* **50** (1989) 1113.
12. A. BHATTACHARJEE and B. MALLIK, *Bull. Chem. Soc. Jpn* **64** (1991) 3129.
13. K.-J. EULER, R. KIRCHHOFF and H. METZENDORF, *Mater. Chem.* **4** (1979) 611.
14. T. N. MISRA, B. ROSENBERG and R. SWITZER, *J. Chem. Phys.* **48** (1968) 2096.
15. B. MALLIK, A. GHOSH and T. N. MISRA, *Proc. Indian Acad. Sci. (Part I)* **88A** (1979) 25.
16. *Idem, Bull. Chem. Soc. Jpn* **52** (1979) 2091.
17. H. WATANABE, I. MOTOYAMA and K. HATA, *ibid.* **39** (1965) 850.
18. B. KARVALY, B. MALLIK and G. KEMENY, *J. Chem. Soc. Farad. Trans. I* **81** (1985) 1939.
19. G. A. SAMARA and H. G. DRICKAMER, *J. Chem. Phys.* **37** (1962) 474.
20. H. A. POHL, A. REMBAUM and A. HENRY, *J. Am. Chem. Soc.* **8** (1962) 2699.
21. M. R. BOON, *Phys. Status Solidi (b)* **51** (1972) K55.
22. A. K. BANDOPADHAY, S. CHATTERJEE, S. V. SUBRAMANYAN and B. R. BULKA, *Mater. Sci.* **7** (1981) 97.
23. M. BATLEY and L. E. LYONS, *Aust. J. Chem.* **19** (1966) 345.
24. B. ROSENBERG, T. N. MISRA and R. SWITZER, *Nature* **217** (1968) 5127.
25. H. G. DRICKAMER and C. W. FRANK, "Electronic Transition and the High Pressure Chemistry of Solids" (Chapman and Hall, London, 1973) p. 100.
26. F. GUTMANN and L. E. LYONS, "Organic Semiconductor", Part A (Wiley, New York, 1967) p. 497.
27. E. POSTOW and B. ROSENBERG, *Bioenergetics* **1** (1970) 467.
28. M. F. DANIEL, A. J. LEADBETIER and M. A. MAJID, *J. Chem. Soc. Farad. Trans. 2* **77** (1981) 1837.
29. K. SATO, M. KATADA, H. SANO and M. KONNO, *Bull. Chem. Soc. Jpn* **57** (1984) 2361.
30. K. IWAI, M. KATADA, I. MOTOYAMA and H. SANO, *ibid.* **60** (1987) 1961.
31. M. F. DANIEL, A. J. LEADBETIER, R. E. MEADS and W. G. ERKER, *J. Chem. Soc. Farad. Trans. 2* **74** (1978) 456.
32. F. GUTMANN, H. KEYZER and L. E. LYONS, "Organic Semiconductor", Part B (Krieger, Malabar, FL, 1983) p. 219.
33. J. C. MEDINA, C. LI, S. G. BOTT, J. L. ATWOOD and G. W. GOKEL, *J. Am. Chem. Soc.* **113** (1991) 366.
34. F. M. COLOMBO, C. D. RAU and V. A. PARSEGIAN, *Science* **256** (1992) 655.
35. F. P. BUNDY, *Phys. B* **139/140** (1986) 390.

Received 5 January
and accepted 21 June 1993